Chemical Research in Toxicology

Article

Cite This: Chem. Res. Toxicol. 2020, 33, 271−280

pubs.acs.org/crt

Can Transcriptomic Profiles from Cancer Cell Lines Be Used for Toxicity Assessment?

Zhichao Liu,*[,†] Liyuan Zhu,[†] Shraddha Thakkar,[†] Ruth Roberts,[‡,§] and Weida Tong*[,†]

[†]National Center for Toxicological Research, U.S. Food and Drug Administration, Jefferson, Arkansas 72079, United States

[‡]ApconiX, BioHub at Alderley Park, Alderley Edge SK10 4TG, U.K.

[§]University of Birmingham, Edgbaston, Birmingham B15 2TT, U.K.

Supporting Information

ABSTRACT: *In vitro* toxicogenomics (TGx) has the potential to replace or supplement animal studies. However, TGx studies often suffer from a limited sample size and cell types. Meanwhile, transcriptomic data have been generated for tens of thousands of compounds using cancer cell lines mainly for drug efficacy screening. Here, we asked the question of whether these types of transcriptomic data can be used to support toxicity assessment. We compared transcriptomic profiles from three cancer lines (HL60, MCF7, and PC3) from the CMap data set with those using primary hepatocytes or *in vivo* repeated dose studies from the Open TG-GATEs database by using our previously reported pair ranking (PRank) method. We observed an encouraging similarity between HL60 and human primary hepatocytes (PRank score = 0.70), suggesting the two cellular assays could be potentially interchangeable. When the analysis was limited to drug-induced liver injury (DILI)-related compounds or genes, the cancer cell lines exhibited promise in DILI assessment in comparison with conventional TGx systems (i.e., human primary hepatocytes or rat *in vivo* repeated dose). Also, some toxicity-related pathways, such as PPAR signaling pathways and fatty acid-related pathways, were preserved across various assay systems, indicating the assay transferability is biological process-specific. Furthermore, we established a potential application of transcriptomic profiles of cancer cell lines for studying immune-related biological processes involving some specific cell types. Moreover, if PRank analysis was focused on only landmark genes from L1000 or S1500+, the advantage of cancer cell lines over the TGx studies was limited. In conclusion, repurposing of existing cancer-related transcript profiling data has great potential for toxicity assessment, particularly in predicting DILI.

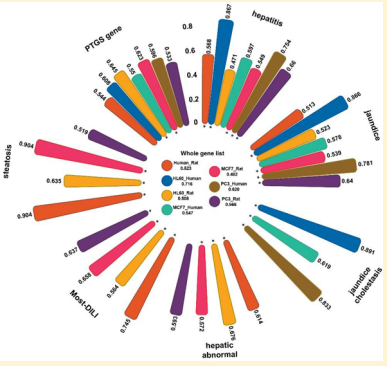

INTRODUCTION

The use and design of animal models for predicting human safety are under constant scrutiny.[1,2] Consequently, a strategic shift away from animal use in risk assessment is underway at the global regulatory agencies. Notably, European Registration, Evaluation, Authorization, and Restriction of Chemicals (REACH) and the European Partnership for Alternative Approaches to Animal Testing (EPAA) have promoted the application of 3Rs principles (replacement, reduction, and refinement of animal testing) in regulatory compliance, communication, and dissemination.[3] In the United States, notable initiatives include Advancing Regulatory Sciences led by the Food and Drug Administration (FDA)[4] and the Tox21 and ToxCast programs initiated by federal agency collaboration.[5,6] These programs facilitate the advancement of applying alternative risk assessment strategies and mechanism-driven methodologies, including *in vitro* and computational approaches, for toxicity assessment of compounds that are important to public health.

Toxicogenomics (TGx), as a maturing discipline, integrates conventional toxicology with genomics technologies to advance risk assessment and drug safety evaluation.[7,8] TGx, especially *in vitro* TGx, has been successfully applied to expand our molecular understanding of toxicological mechanisms and serves as a useful tool in predictive toxicology.[9−11] For example, Li et al.[12] developed a DNA transcriptomic biomarker (TGx-DDI) known as TGx-28.65, which could rapidly distinguish DNA damage-inducing compounds from nongenotoxicants. This biomarker bridges the gap between *in vitro* mutation assays and *in vitro* chromosomal damage assays with respect to throughput.

Like conventional toxicology approaches, there are many variables in the design of TGx experiments such as the choice of species, cell types of studying, time of exposure, dose/concentration, and route of administration. With a broad range of available TGx approaches and methodologies, which is the optimum approach to use for which toxicological end points? For example, in the context of TGx, what are the differences among various preclinical models? Can a 1-day single-dose experiment replace a 28-day repeated dosing study? Is it possible to extrapolate from *in vitro* to *in vivo*? What is the

Special Issue: Drug Metabolism and Toxicology

Received: July 17, 2019
Published: December 6, 2019

DOI: 10.1021/acs.chemrestox.9b00288
Chem. Res. Toxicol. 2020, 33, 271−280

critical difference among various animal-free models? To address these questions, we developed a pair ranking (PRank) methodology to analyze different TGx assays from open TG-GATEs and made several observations.[13,14] For example, we observed that the *in vitro* assay using primary rat hepatocytes had a high *in vitro* to *in vivo* extrapolation (IVIVE) potential to a standard 28-day rat *in vivo* repeated dose model for most drug-induced liver injury (DILI) end points, supporting the 3Rs principles.[14] Additionally, we found a good correlation between a short-term *in vivo* single-dose assay and a standard 28-day *in vivo* repeated dose study provides a possible way to conserve resources.[13] In many cases, the interchangeability between the TGx assay systems depends on the toxicity pathway and therapeutic category to be investigated. All of these conclusions provided useful information for positioning *in vitro* TGx approaches in risk assessment. Considering the limited number of compounds tested and the few cell types used in the TGx setting, it is still challenging to fully implement *in vitro* TGx in risk assessment and to realize its role in the regulatory application.

In contrast, transcriptomic profiles of tens of thousands of compounds have been generated using immortalized cell lines (most are cancer cell lines) and successfully applied in drug discovery,[15] drug repositioning,[16] and biomarker discovery.[17] Furthermore, some novel *in vitro* assay platforms such as L1000 and TempO-seq significantly reduce assay screening costs and generate data in a high-throughput manner.[18,19] If gene expression patterns from cancer cell lines could recapitulate the biology noted in standard *in vivo* TGx assays, it would tremendously expand the impact of *in vitro* transcriptomic profiling in risk assessment and safety evaluation. Some initial attempts have been made to repurpose the transcriptomic profiles generated under immortalized cell cultures to capture the similar biological functions generated during *in vivo* TGx assays[20] and to develop computational models.[17]

To further explore the potential of using the transcriptomic profiling assays of cancer cell lines in toxicity assessment, we conducted a comprehensive investigation of the similarity of gene activities between transcriptomic profiles from cancer lines in connectivity map (CMap)[21] and TGx assays in open TG-GATEs[22] using the PRank method. Moreover, the extensive comparisons were conducted by limiting the analyses to the compounds causing DILI and gene sets representing related predictive toxicogenomics space (PTGS), specific toxicology-related pathways, and immune system-related perturbations.

MATERIALS AND METHODS

Cancer Cell Line Genomics Data Sets. CMap 02 was employed as the representative transcriptomic profiling data set of immortalized cell lines.[21] CMap 02 consisted of transcriptomic profiles of 1309 compounds generated in different cancer cell lines with a 6 h treatment duration. Three microarray platforms, including HG-U133A, HT-HG-U133A, and HT-HG-U133A_EA, were used, containing measurements mainly for three cancer cell lines (e.g., HL60, MCF, and PC3) with matched control samples. The raw CELL files can be downloaded from https://portals.broadinstitute.org/cmap/.

The downloaded CELL files were robust multiarray normalized (RMA) with the *affy* package in R Bioconductor. The custom CDF files (version 20) from BRIANARRAY (http://brainarray.mbni.med.umich.edu/Brainarray/Database/CustomCDF/CDF_download.asp) were used to collapse multiple probe sets into a single gene. Only the 12254 common genes among the three microarray platforms were retained. Then, fold change values for each compound in different cancer cell lines were calculated by comparing samples in the treatment group versus the matched control group with the R *limma* package. We excluded treatment instances (compound and cell line pair) with a single matched control sample. Consequently, a total of 3478 treatment instances were generated, which corresponded to 1072, 1255, and 1149 treatment instances in HL60, MCF7, and PC3 cell lines, respectively.

Toxicogenomics Data Sets. Liver-related treatment data from the open TG-GATEs (http://toxico.nibiohn.go.jp/english/) were used in this study,[22] which consist of ∼170 compounds tested in four TGx assays with multiple treatment durations at three different doses (i.e., low, medium, and high) and a time-matched control. These assays are two *in vitro* assays (one applied to primary hepatocytes from Sprague-Dawley rats and the other used the pooled human donors) and two rat *in vivo* assays (i.e., single- and repeated-dosage treatments). In this study, we used the *in vitro* data from human primary hepatocytes (e.g., Human_In_Vitro), which used 24 h treatment durations and a high concentration. We also used the rat *in vivo* repeated dose data with a high dose and longest duration (28 days) that was the standard long-term TGx assay (e.g., Rat_In_Vivo), to investigate the IVIVE potential. Additional details of the study design were described elsewhere.[13,14,22]

Following the same preprocessing procedure used for the CMap data set, the RMA was used to normalize the raw CELL data of Human_In_Vitro and Rat_In_Vivo with custom CDF files *hgu133plus2hsensgcdf* and *rat2302rnensgcdf* version 19, respectively. There are 19363 and 13877 unique genes for each instance [e.g., compound/time/dose (or concentration) combination] obtained for Human_In_Vitro and Rat_In_Vivo, respectively. The 13877 *Rattus norvegicus* Entrez gene IDs in Rat_In_Vivo were further mapped onto *Homo sapiens* Entrez gene IDs based on NCBI HomoloGene build 68 (ftp://ftp.ncbi.nih.gov/pub/HomoloGene/build68/). Then, fold change values were calculated in each compound/time/dose or concentration condition with samples between matched treatment versus the control groups by the R *limma* package. Consequently, there were a total of 156 instances in Human_In_Vitro and 134 instances in Rat_In_Vivo.

We used the 96 overlapping compounds between CMap and the open TG-GATEs for PRank analysis. The 96 common compounds were generated on the basis of their shared parent InChIKeys extracted from https://pubchem.ncbi.nlm.nih.gov/idexchange/idexchange.cgi. More details of the overlapped compounds are listed in Table S1.

Drug-Induced Liver Injury Annotation. The 22 drug-induced liver injury (DILI) end points were annotated and curated in our previous study.[14] We further matched the compounds in each DILI end point with the 96 common compounds shared by CMap and TG-GATEs data sets. Consequently, six DILI end points were selected, including hepatitis, jaundice, jaundice cholestasis, hepatic function abnormal, Most-DILI concern, and steatosis, with >20 compounds for further analysis. Furthermore, a list of 1331 genes derived from transcriptomics data representing a "predictive toxicogenomics space" (PTGS) was used for assay concordance analysis (see Table S2). The details of the PTGS gene set generation were described elsewhere.[17]

To investigate whether the *in vitro* cell lines are able to distinguish *in vivo* hepatotoxicants from nonhepatotoxicants, the SIDER4 database (http://sideeffects.embl.de/)[23] that contains information about marketed medicines and their recorded adverse drug reactions (ADRs) was employed. The adverse drug reactions in the SIDER4 database are coded by the Medical Dictionary for Regulatory Activities (MedDRA). First, we mapped 96 overlapped compounds onto the 1430-drug list in the SIDER4 database and extracted their related adverse drug reactions [low-level terms (LLTs) in MedDRA]. Then, we mapped these low-level terms (LLTs) onto the system organ class (SOC) level. We kept the LLTs not belonging to "hepatobiliary" in the SOCs, which were considered as non-liver-related ADRs. Similarly, we kept only the ADR with >20 drugs for

DOI: 10.1021/acs.chemrestox.9b00288
Chem. Res. Toxicol. 2020, 33, 271−280

further analysis. As a result, we obtained 15 non-liver-related ADRs (see Table S3).

Toxicity Pathway-Related Gene Sets. Toxicity pathway-related gene sets were curated from the Comparative Toxicogenomics Database (CTD, http://ctdbase.org/), which aims to delineate how the environmental exposures affect public health.[24] The gene−pathway association data set was downloaded from http://ctdbase.org/downloads/ (data acquired June 25, 2018). There were a total of 135804 gene−pathway relationships, which corresponded to 11586 human genes and 2363 toxicity-related pathways. We retained 120 toxicity pathways with >200 genes for further analysis.

Immune Cell Gene Signatures. Immune cell gene expression data in mouse cell lines and tissues were extracted from the Immunological Genome Project (ImmGen).[25] The preprocessing and normalization of data were described previously.[26,27] Specifically, 304 differential state gene expressions (e.g., fold change values) covering 11153 mapped ortholog human Entrez gene ids were generated between two steady state profiles from 221 unique immunological cell types. In this study, we ranked gene expression profiles from high to low based on fold change values for each of the 304 immune-related states. Then, the top/down 500 genes in each immunological state were selected as the differentially expressed gene (DEG) signature for further analysis.

L1000 Landmark Gene Sets. The NIH Library of Integrated Network-Based Cellular Signatures (LINCS) 1000 project developed a novel, low-cost, and high-throughput reduced representation expression profiling approaches based on 978 landmark gene sets. The rationale behind the L1000 landmark gene set concept was that the gene expression was highly correlated, and the selected 978 landmark gene sets could recapture the biology and represent the whole genome-wide expression. The 978-landmark gene set was downloaded from https://www.ncbi.nlm.nih.gov/geo/query/acc.cgi?acc=GPL20573 (Table S4).

S1500+ Affymetrix Gene Sets. Like the concept of the L1000 landmark gene set, Tox21 developed an S1500+ "sentinel" gene set based on the Affymetrix microarray platform (HG-U133plus2) to represent all known canonical pathways from the Molecular Signature Database (MSigDB version 4.0) and to infer expression changes for the remaining transcriptome.[28] The S1500+ gene set, including 2753 unique human genes, was employed for further analysis (Table S5).

PRank Methodology. The PRank method was developed and successfully used to assess the extrapolation potential among TGx assays.[13,14] The PRank method provided a solution to compare any two assay systems consisting of the following three steps.

(1) Compound Pairwise Similarity. For each assay system, the compound pairwise similarity between any two compounds was calculated on the basis of their shared significant genes. First, the significant genes of each compound were generated by extracting top N upregulated and downregulated genes from ranked fold change values. In our previous study, we selected the top 200 up/downregulated genes in TGx assays, which generated enough discrimination power to distinguish the transcriptomic profiles. In this study, we optimized the number of genes for CMap data based on the stability of ranked similarity lists generated on the basis of a different number of genes, as proposed in our previous study.[14] Then, Dice's coefficient between the significant genes of compounds was calculated by considering the gene regulation directions.

For pairwise similarity measurement using different gene sets, we kept only mapped genes with fold changes of >1.5 to calculate the similarity in our previous study.[13] It tended to cause the limited mapped genes for similarity calculation. Therefore, we updated the similarity measurement by using the following strategies. First, we mapped the significant genes of compounds onto each gene set described in the subsections above. Then, we used the Pearson's correlation coefficients to calculate the compound pairwise similarity by using R function *cor*.

(2) Rank-Order Compound Pairwise Similarity. The compound pairwise similarities were arranged in decreasing order for each assay system.

(3) PRank Score Calculation. PRank score was calculated on the basis of the area under the curve (AUC) value from a receiver operating characteristic (ROC) curve analysis, which was employed to measure the preservation of ranked similarity list from one testing system to the other. The ROC-AUC analysis requires a "ground truth" with binary representation. Therefore, we needed to translate the targeted ranked similarity list to positive and negative values (e.g., 1 or 0). On the basis of the distribution of ranked similarity list, we selected the Dice's coefficient of a >99.5% quantile as a cutoff to identified positive compound pairs. The ROC-AUC analysis was conducted using R *pROC* packages.

Pattern Analysis of Gene Expression and Functional Analysis. For each assay system, we ranked significant genes on the basis of their expressed frequency across all of the compounds. Then, we selected the 500 most frequently expressed genes in each assay system to calculate their percentage of overlapping genes (POGs). The details of the POG calculation could be found in our previous study.[13] For genes involved in the specific pathway, we extracted the most frequently expressed genes in the pathway across all of the compounds and then carried out the comparative analysis among the different cell-based *in vitro* assays.

The KEGG pathway analysis was conducted with the 400 most frequent genes in each assay system by using the Database for Annotation, Visualization and Integrated Discovery (DAVID) software.[29] The enriched pathways with a Benjamini−Hochberg adjusted p value of <0.05 were considered as statistically significant pathways.

Chemical Structure Similarity. The chemical structures (Canonical SMILES) of common compounds were downloaded from https://pubchem.ncbi.nlm.nih.gov/pc_fetch/pc_fetch.cgi. Then, the compound pairwise chemical structure similarity was calculated on the basis of their functional class fingerprints (FCFPs) with a radius of FCFP-4 by using Pipeline Pilot 8.0 (Accelrys, Biovia, and, Dassault Systems) (Table S6).

Code Availability. The scripts and processed data in this study are available at https://www.synapse.org/#!Synapse:syn20505083/files/

RESULTS

Optimized Number of Genes. We first optimized the number of genes to represent the compounds for pairwise similarity calculation. The detailed strategies for determining the number of genes were described in our previous study.[14] Briefly, we incrementally increased the number of genes by 50, and the correlation between before and after incrementation for the rank order of drug pairs was calculated. Figure 1 depicts

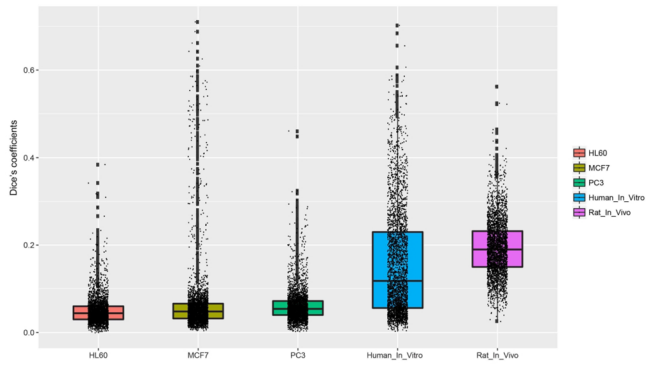

Figure 1. Stability of ranked similarity list for each assay system. The data points denote the Spearman's correlation coefficients for HL60 (red), MCF7 (dark yellow), PC3 (green), Human_In_Vitro (blue), and Rat_in_Vivo (purple), which were calculated by comparing the ranked similarity list with different numbers of DEGs with R function *cor*.

DOI: 10.1021/acs.chemrestox.9b00288
Chem. Res. Toxicol. 2020, 33, 271−280

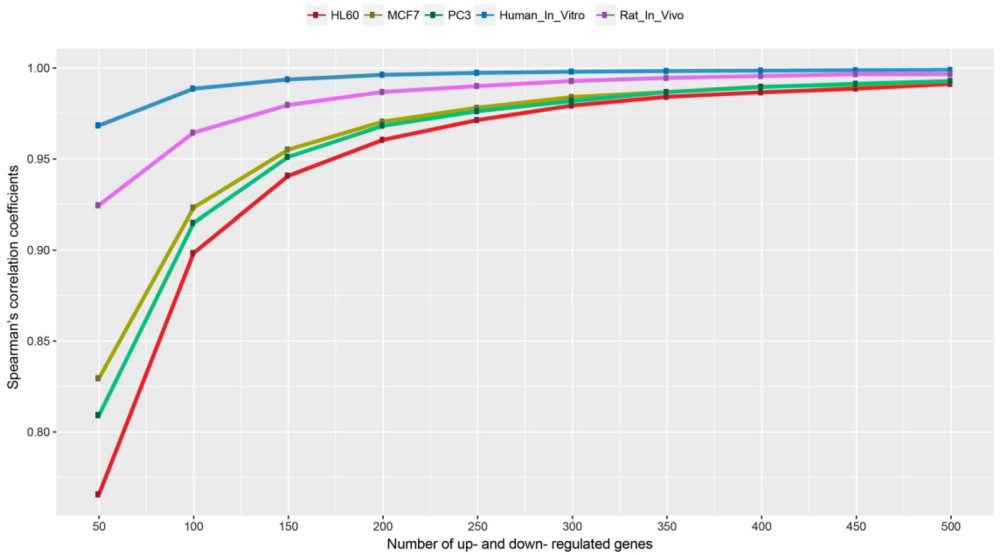

Figure 2. Distribution of compound pairwise similarity in each assay system. Compound pairwise similarity was generated by using Dice's coefficients. Dice's coefficients were calculated on the basis of the top up/down 250 genes ranked by fold changes for any two compounds in each system.

the change of Spearman's correlation coefficients with the incremental number of significant genes for five different assay systems (e.g., HL60, MCF7, PC3, Human_In_Vitro, and Rat_In_Vivo). The Spearman's correlation coefficients tended to be stable with more than 250 up- and downregulated genes in all five assay systems. Furthermore, two TGx assay systems (e.g., Human_In_Vitro and Rat_In_Vivo) had Spearman's correlation coefficients higher than those of cancer cell line-based assays (e.g., HL60, MCF7, and PC3), suggesting that the TGx assay systems were less sensitive to the number of genes used to rank-order compound pairs with respect to the cancer cell lines. Therefore, the top 250 up- and downregulated genes of each compound were selected as signatures for the similarity calculation.

Discriminatory Power of the Assays. We calculated Dice's coefficients for each assay where a low coefficient indicates a stronger ability to differentiate compound pairs from one another. Figure 2 shows the distribution of compound pairwise similarity in each assay system. The average and standard deviation of Dice's coefficients were ranked in the following order: Rat_In_Vivo (0.1935 ± 0.0637), Human_In_Vitro (0.1564 ± 0.1212), MCF7 (0.0662 ± 0.0823), PC3 (0.0611 ± 0.0375), and HL60 (0.0493 ± 0.0308). This indicates that the cancer cell line-based assays demonstrated a stronger ability to differentiate compound pairs. For the MCF assay, the standard deviation of Dice's coefficients is larger than the average value, indicating the high variability of pairwise similarity. Furthermore, the ranked assays based on the difference between the maximum and average of Dice's coefficients (i.e., a maximum of Dice's coefficients − average Dice's coefficients) were as follows: Human_In_Vitro (0.5456), MCF7 (0.6437), PC3 (0.3989), Rat_In_Vivo (0.3684), and HL60 (0.3347). Thus, high-similarity compound pairs were distinguished more easily during *in vitro* assays (except HL60 and PC3) than in the *in vivo* assay system.

In the previous study, we investigated the discriminatory power of TGx assays for use in chemical structure-based read-across, suggesting that combining two types of information improves read-across performance.[13,14] Here, we further investigated whether the transcriptomic profiles from cancer cell lines would add value to the chemical structure-based read-across approach. We found that the Pearson's correlation coefficients of compound pairwise similarity were very low (e.g., 0.224, 0.189, and 0.210) between chemical spaces and transcriptomic profiles of three cancer cell lines (HL60, MCF7, and PC3, respectively). The low correlations between chemical and transcriptomic space suggested that the improved chemical-based read-across performance may be warranted when integrating with transcriptomic information about cancer cell lines.

Comparison of TGx Study Designs with Cancer Cell Line-Based Drug Transcriptomic Profiles. Figure 3 summarizes PRank scores of three cancer cell line assays (HL60, MCF7, and PC3) against two TGx assays (Human_In_Vitro and Rat_In_Vivo), along with the scores among

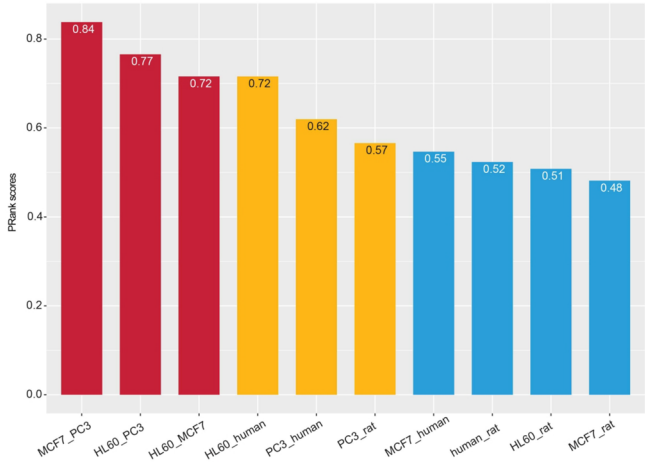

Figure 3. Concordance between assay systems based on PRank scores. PRank score was calculated by using ROC-AUC analysis. The box plot was divided into three parts: the high, moderate, and low PRank scores colored red, yellow, and blue, respectively.

DOI: 10.1021/acs.chemrestox.9b00288
Chem. Res. Toxicol. 2020, 33, 271−280

three cancer cell lines. The higher concordances among assay systems were observed among three cancer cell lines assays (MCF7 vs PC3, HL60 vs PC3, and HL60 vs MCF7) with PRank scores of 0.84, 0.77, and 0.72, respectively (red in Figure 3). The moderate concordances (yellow in Figure 3) were obtained for HL60 versus Human_In_Vitro (PRank score of 0.72) and PC3 versus Human_In_Vitro (PRank score of 0.62), indicating that the transcriptomic profiles of cancer cell lines were somewhat similar to those of human primary hepatocytes and could be useful for assessing DILI. However, the concordance in transcriptomic expression between human cancer cell lines and rat primary hepatocytes was low (blue in Figure 3)..

To further verify the findings, we carried out a percentage of overlapping genes (POG) analysis based on the 500 most frequently expressed genes of compounds in each assay system (detailed in Materials and Methods). The POG curves of any two assays were consistent with the PRank findings (Figure S1). However, the PRank method had better resolution to distinguish assay systems (e.g., HL60 vs Human_In_Vitro and PC3 vs Human_In_Vitro) with moderate concordance than that of the POG method. We further conducted the KEGG pathway analysis obtained from the 500 most frequently expressed genes in each assay system. The overlapped significant pathways are shown in a Venn diagram (Figure S2). Some pathways such as the PPAR signaling pathway (KEGG id: hsa03320) and the FoxO signaling pathway (KEGG id: hsa04068) were significantly enriched (with adjusted p values of <0.05) by the 500 most frequently expressed genes from PC3, Human_In_Vitro, and Rat_In_Vivo, suggesting that the IVIVE potential (e.g., immortalized cell lines and Rat_In_Vivo) could be enhanced in some specific pathways or biological processes.

Application in Drug-Induced Liver Injury (DILI). DILI is one of the main reasons for the failure of drug candidates in the late stages of clinical trials.[30] The TGx data in this study are derived from the liver, which offers an opportunity to assess the potential of cancer cell lines for DILI prediction by comparing it with liver-specific TGx studies. We conducted PRank analysis by limiting compounds causing DILI and using a list of reported genes related to DILI predictive toxicogenomics space (PTGS).[17]

Six DILI end points, including hepatitis, jaundice, jaundice cholestasis, hepatic function abnormal, Most-DILI concern, and steatosis, were employed. We observed that, by comparing Rat_In_Vivo and Human_In_Vitro, three cancer lines displayed improved PRank scores for six DILI-specific end points. A total of 72.4% of PRank scores were improved by 10% in comparison to the whole compound list (marked with an asterisk in Figure 4A). Notably, the concordance for Most-DILI concern and jaundice cholestasis was improved for all of the assay comparisons. To further investigate the ability of *in vitro* cell lines to distinguish *in vivo* hepatotoxicants from nonhepatotoxicants, we compared six DILI-specific end points to 15 non-liver-related adverse drug reactions (ADRs) (see Table S3). We found the PRank scores of DILI-specific end points are larger than most of those of non-liver-related ADRs between HL60 and Human_In_Vitro, indicating the potential discriminative power of a specific cancer cell line (i.e., HL60) to differential DILI from non-DILI compounds (Figure 4B).

PTGS consisted of 1331 genes that were distributed over 14 cytotoxicity-related gene spaces and served as "sentinel" genes for DILI prediction. The concordance among assay systems

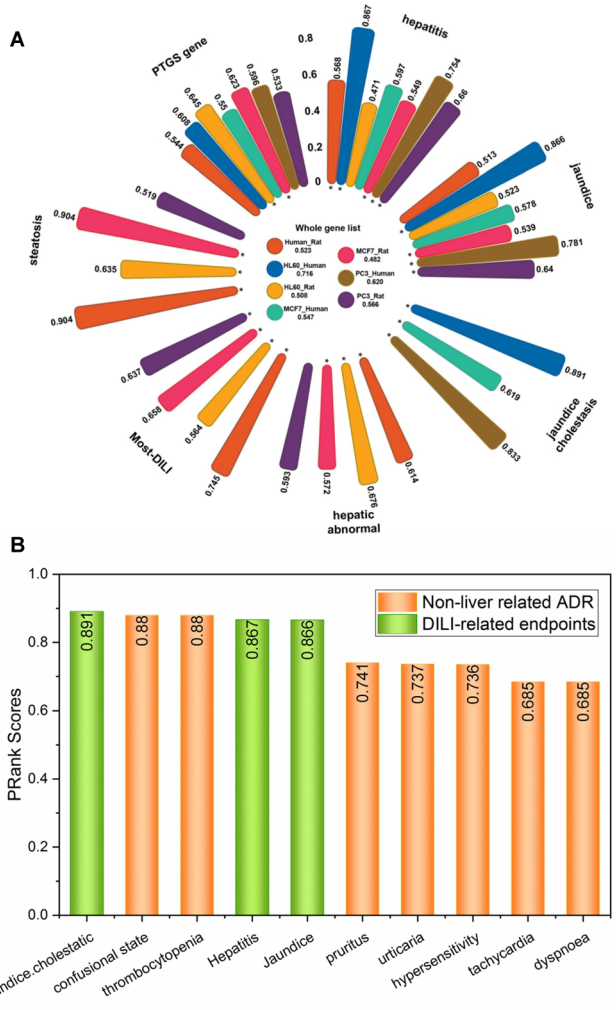

Figure 4. (A) Distribution of PRank scores for DILI-related annotation among transcriptomic profiling assay systems. The DILI annotation data consisted of six DILI end points and a list of genes representing DILI predictive toxicogenomics space (PTGS). The six DILI end points included hepatitis, jaundice, jaundice cholestasis, hepatic function abnormal, Most-DILI concern, and steatosis. The PRank scores for different DILI annotation data were depicted by using a circle box plot. Meanwhile, PRank scores with all of the compounds studied are listed in the middle. The bars with asterisks indicate that their corresponding Prank scores were increased by 10% in comparison to that of the whole list used. The PRank scores of the full compound list are listed in the middle of the circle box plot. (B) PRank scores between HL60 and Human_In_Vitro for DILI end points and non-liver-related ADR: DILI-related end points (green) and non-liver-related ADRs (orange).

was further assessed by comparing the expression pattern of 1331 PTGS genes with the PRank method (Figure 4A). The concordances of HL60 versus Rat_In_Vivo (PRank score of 0.645) and MCF7 versus Rat_In_Vivo (PRank score of 0.623) were marginally increased by 10% in comparison to the whole gene list studied. However, the PRank scores among HL60, PC3, and Human_In_Vitro were dramatically decreased, implying the specific DILI-related biological process perturbed by different *in vitro* assay systems.

Toxicity Pathways. We further investigated the concordance between TGx assays and cancer cell line assays when limiting the genes to specific toxicity-related pathways. The analysis was focused on 120 toxicity-related pathways obtained

DOI: 10.1021/acs.chemrestox.9b00288
Chem. Res. Toxicol. 2020, 33, 271−280

from CTD that involved more than 200 genes. In Figure 5, the stacked areas are arranged in decreasing order based on the

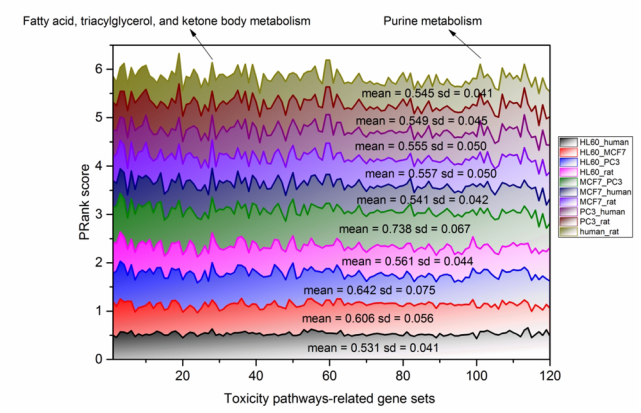

Figure 5. Concordance among transcriptomic profiling assay systems for gene sets related to different toxicity-related pathways. The stacked plots of PRank scores for different gene sets in the assay systems. A total of 120 toxicity-related pathways with more than 200 genes involved from the Comparative Toxicogenomics Database (CTD, http://ctdbase.org/) were employed. The average and standard deviation values of PRank scores of 120 toxicity-related pathways in each assay comparison are illustrated.

average value of PRank scores of 120 toxicity-related pathways. The ranked average PRrank scores between assay pairs were consistent with the whole gene studied. Several top-ranked toxicity-related pathways based on PRank scores such as fatty acid, triacylglycerol, and ketone body metabolism and purine metabolism were consistently enriched across the assay systems, which further confirmed our findings that assay transferability was dependent on the biological pathway.[13] To further investigate the similarity and differences of expressed genes in the two pathways (i.e., fatty acid, triacylglycerol, and ketone body metabolism and purine metabolism), we carried out a comparative analysis of the most frequently expressed genes of drugs between cancer cell lines (i.e., HL60/PC3/MCF7) and TGx assays (i.e., human primary hepatocytes and rat liver). It was found that approximately the commonly expressed genes occupied approximately 17−19.9% and 11.3−15.6% of all of the expressed genes in the three assay systems (i.e., cancer lines, Rat_In_Vivo, and Human_In_Vitro) for the two pathways (see Figure S3 and Table S7). These common genes may provide useful information about IVIVE potential. Moreover, the results here are complementary with the KEGG pathways mentioned above; it was reported that PPARs made up a unique set of fatty acid-regulated transcription factors controlling both lipid metabolism and inflammation.[31]

Immune-Specific Genes. One of the greatest challenges for an *in vitro* system in toxicity assessment is to model the immune-related characteristics of *in vivo* organisms in an *in vitro* environment.[32] For that, we limited the analysis of 1000 genes (top up and down 500 differentially expressed genes) for each of the 304 immune-related states. PRank scores of 304 immune-related states across different assay systems are listed in Table S8. Figure 6 provides PRank scores for the top five immune-related cell types among different assay pairs. We observed that the gene expression pattern of immune-related cell types tended to be preserved in different transcriptomic profiling assays. For example, T gamma delta (Tgd) cells are

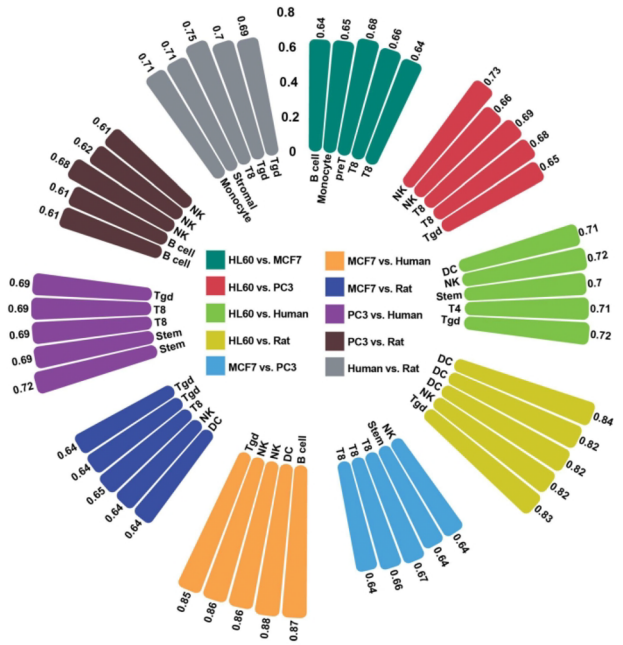

Figure 6. Distribution of top-ranked PRank scores for differentially expressed genes (DEGs) of different immune-related states among transcriptomic profiling assay systems. A total of 304 immune system-related states were assessed with the PRank method among the assay systems. The top five ranked PRank scores related to immune cells are plotted in circle bars. The full ranking list of immune-related states based on PRank score can be found in Table S10.

well-maintained between MCF7 versus Rat_In_Vivo and HL60 versus Rat_In_Vivo assays, suggesting the potential application of transcriptomic profiling assays in cancer cell lines for studying the immune-related biological process involving Tgd cells. Another example is natural killer (NK) cells, which are the type of lymphocytes involved in host rejection of both tumors and virally infected cells. The transcriptional properties of NK cells were well preserved across different assay systems. We also found that gene expression patterns of T8 lymphocytes (T8) were well preserved within transcriptomic profiles of cancer cell lines (i.e., HL60, MCF7, and PC3).

Landmark Genes. The concept of landmark genes that represents the predominant biology at the whole genome scale offers an opportunity to develop manageable high-throughput screening assays at a low cost. Two representative landmark gene sets, L1000 landmark genes with 978 genes[19] and Affymetrix S1500+ with 2735 genes,[28] were used to assess the cancer cell line-based transcriptomic profiling with respect to TGx assays. Compared with the concordance with all of the compounds studied, the decreased PRank scores of most assay comparisons were observed when using S1500+ and L1000 landmark gene sets. Of note, the PRank of MCF versus Rat_In_Vivo was improved dramatically by 33.6% (from 0.482 to 0.644), demonstrating a divergence of preserved gene expression patterns in different cancer cell lines (Figure 7).

DISCUSSION

Challenges encountered in interpreting animal studies to predict human toxicity have stimulated many to rethink and reevaluate alternative strategies for risk assessment. The strategic shift to the use of *in vitro* assays assisted by computational approaches holds promise for reinvigorating

DOI: 10.1021/acs.chemrestox.9b00288
Chem. Res. Toxicol. 2020, 33, 271−280

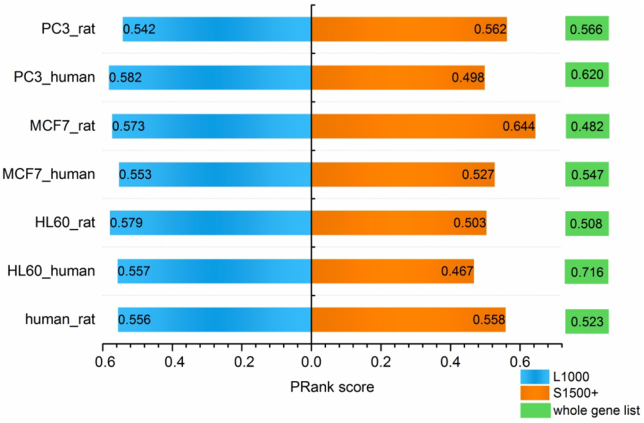

Figure 7. Concordance among transcriptomic profiling assay systems for landmark gene sets. Two landmark gene sets, including 978 L1000 landmark genes and 2753 S1500+ landmark genes, were used. PRank scores are plotted as bars and colored blue, orange, and green for the L1000, S1500+, and whole gene list, respectively.

this risk assessment paradigm. Transcriptomic profiling of immortalized cell lines has led to the accumulation of vast numbers of data points en route to improving our understanding of cancer pathogenesis and oncology drug development.[33,34] However, whether these data could be applied to understanding toxicology or to the assessment of toxicological hazard or risk is still unclear.

To address these unanswered questions, we conducted a comprehensive analysis of the concordance between cancer cell line-based transcriptomic profiling assays and TGx assay systems. Some encouraging results were obtained, which could serve as a foundation for the selection of immortalized cell lines to further develop predictive models in toxicology. Overall, excellent PRank scores were captured within transcriptomic profiling assays of cancer cell lines. The correlation between *in vitro* assay systems suggested *in vitro* TGx and specific cancer cell line-based transcriptomic profiling assays (i.e., HL60) could be interchangeable. Primary human hepatocyte cultures have been considered as the gold standard for the creation of human-relevant liver cell culture models. Moreover, they present significant and predictive results in pharmacological and toxicological *in vitro* research due to their unstable differentiation.[35] Hepatocytes are differentiated cells expressing many hepatic functions and retain the expression of both Phase I and II enzymes for a limited time in culture. Thus, tests on primary hepatocyte cultures are often capable of elucidating mechanisms of DILI. For example, many drugs inducing severe DILI have been shown to cause an elevated ROS/ATP ratio in primary human hepatocyte cultures, indicating oxidative stress.[36]

However, the extrapolation from *in vitro* to *in vivo* was poor, indicating that species differences contributed to the large divergence between assay systems. Furthermore, we noticed that the correlation between the human primary hepatocytes and MCF cells was also suboptimal, suggesting that something other than species may be driving the different responses between cancer cell lines and normal human hepatocytes and rat tissue. Therefore, a closer investigation of the TGx assay and different cancer lines beyond the data employed in this study was strongly recommended.

Moreover, the gene expression of compounds in different assay systems is multifactorial. Due to limitations of the data, some important variables and factors that potentially impact the transcriptomic response in different cell cultures are not included in this study. For example, factors such as the passage number, de-differentiation of cancer cell lines, and the time of treatment after plating cells are not taken into consideration. Furthermore, the interior difference among the cancer cell lines (i.e., HL60 cells are suspended hematological cells, whereas MCF-7 cells are adherent monolayer-transformed mammary epithelial cells that lose estrogen receptor signaling with an increasing passage number) and different culture conditions (i.e., medium/serum) is strongly recommended to further verify and correct the findings based on the limited data in this study.

DILI is a complex clinical end point and poses a challenge to the pharmaceutical industry and to regulatory agencies due to inadequate methods of prediction.[37−39] Many DILI prediction models have been developed on the basis of information such as chemical structures,[40−42] toxicogenomics profiles,[43] and high-throughput screening (HTS) assays.[44] These models have improved DILI management to some extent. However, many of these DILI prediction models suffer from insufficient data points, and their power is too limited for clinical application. The initial findings of our analysis may provide useful information and pave the way for further investigation of the potential to reuse transcriptomic profiling assays of cancer cell lines for the prediction of DILI.

The transferability among assays improves when the focus is on specific pathways related to bioenergetics. The phenomenon of specific pathways related to bioenergetics perturbation was preserved across the transcriptomic profiling assay systems. In our previous study, we found that the same compound could perturb fatty acid-related pathways (e.g., fatty acid, triacylglycerol, and ketone body metabolism and purine metabolism) and PPAR signaling pathways across TGx assay systems.[13,14] Here, we further confirmed the preservation of these pathways in the transcriptomic profiling assay of cancer cell lines. The finding also demonstrated the possibility of repurposing cancer cell line transcriptomic profiles for risk assessment.

One of the criticisms of *in vitro* assays is their poor recapitulation ability of immune-related characteristics in organisms, leading to limited predictive power for human toxicity.[45] Arguably, a key aspect of the toxicological response *in vivo* is adaptation and recovery, which to a large extent involves immune-related biological processes. The representation of immune-related properties differs in different cell types. For example, HL-60 cells are neutrophil-like leukemia cells, which potentially should be more accurate at picking up immune-related mechanisms than MCF7 or PC3 cells. However, further investigation of the correlation between the gene activity represented in the cancer cells and immune cells is still an open question. Therefore, a comprehensive assessment of the preservation of immune-related features in different assay systems is urgently needed to assess the suitability for these assays in risk assessment

Several scientific communities and government-led initiatives have utilized the concept of landmark genes to develop affordable high-throughput transcriptomic (HTT) methods, allowing for the screening of larger numbers of untested samples.[19,28] Due to the heterogeneity of the cell types used, one critical question is how to select the "fit-for-purpose" cell types for *in vitro* assay development. An analysis was conducted and suggested the possibility of repurposing cancer cell lines

DOI: 10.1021/acs.chemrestox.9b00288
Chem. Res. Toxicol. 2020, 33, 271−280

based on transcriptomic profiling assays for DILI prediction with an improved prediction performance. We observed low PRank scores (<0.6) among the assay systems when limiting the comparison with L1000 and S1500+ landmark genes, which projected the complexity of gene expression patterns regulated in a coordinated fashion under different assay systems. The extrapolation power of these landmark gene sets in various *in vitro* assay systems offers an opportunity to implement landmark gene-based HTS assays for risk assessment and requires further investigation.

The PRank method provided an innovative strategy for assessing transferability between transcriptomic profiling assays. The PRank method hypothesizes that the ranking of transcriptomic profile similarity between compounds could be preserved if the two assay systems are interchangeable. The PRank aims to provide a framework for assay comparison. Any advanced methods could be injected into the frame for better performance. For example, we employed Dice's coefficients for compound similarity calculation. Other measurement strategies, including the Jaccard index, K-L divergence based on the distribution of topics derived from the Latent Dirichlet allocation (LDA) models, are the alternative options for pairwise similarity calculation. Furthermore, the PRank score was calculated on the basis of the AUC value from ROC-AUC analysis. The binary cutoff should be determined and is currently based on an arbitrary determination. Some nonparametric vector ranking comparison strategies were encouraged to provide a more objective measurement. Along with our two previous studies, we comprehensively assessed some influential factors of the PRank method such as preprocessing procedures (e.g., FAMERS, MAS5, and RMA), the optimized number of DEG, and multiple time/dose combinations. It was demonstrated that the PRank method could provide a reliable solution for transcriptomic assay comparison to guide assay selection in risk assessment and drug safety evaluation.

■ ASSOCIATED CONTENT

Supporting Information

The Supporting Information is available free of charge at https://pubs.acs.org/doi/10.1021/acs.chemrestox.9b00288.

Information about 96 common compounds among the *in vitro* assay systems (Table S1) (XLSX)

Predictive toxicogenomics space (PTGS) gene list (Table S2) (XLSX)

PRank scores for DILI end points and nonrelated ADRs (Table S3) (XLSX)

L1000 gene list (Table S4) (XLSX)

S1500+ gene list (Table S5) (XLSX)

Pairwise compound similarity based on functional class fingerprints (FCFPs) (Table S6) (XLSX)

The most frequent genes among cancer cell lines (i.e., HL60, PC3, and MCF7) and TGx assays (i.e., Human_In_Vitro and Rat_in_Vivo) for two lipid-related pathways, including fatty acid, triacylglycerol, and ketone body metabolism and purine metabolism (Table S7) (XLSX)

PRank scores for differentially expressed genes (DEGs) of different immune-related states among transcriptomic profiling assay systems (Table S8) (XLSX)

Percentage of overlapping genes between any two transcriptomic profiling assays. For each assay system, we ranked significant genes on the basis of their expressed frequency across all of the compounds. Then, we selected 500 most frequently expressed genes in each assay system to calculate their POG values. The POG value were calculated with the overlapped genes between any two assay systems dividing the number of most frequently expressed genes investigated (Figure S1) (TIF)

Venn diagram of overlapping KEGG pathways in the transcriptomic profiling assay. The KEGG pathways were enriched with the 500 most frequently expressed genes in each assay system by using the Database for Annotation, Visualization and Integrated Discovery (DAVID: https://david.ncifcrf.gov/). The KEGG pathways were adjusted, and p values of <0.05 were selected as statistically significant pathways (Figure S2) (TIF)

Venn diagram of the most frequent genes among cancer lines (i.e., HL60, PC3, and MCF7) and TGx assays (i.e., Human_In_Vitro and Rat_in_Vivo) for two lipid-related pathways (Figure S3) (TIF)

■ AUTHOR INFORMATION

Corresponding Authors

*E-mail: zhichao.liu@fda.hhs.gov.

*E-mail: weida.tong@fda.hhs.gov.

ORCID

Zhichao Liu: 0000-0002-5376-9003

Weida Tong: 0000-0002-4093-3708

Author Contributions

Z.L. and W.T. conceived and designed the experiments. Z.L. analyzed the data and the first version of the manuscript. Z.L. contributed reagents, materials, and analysis tools. Z.L., S.T., R.R., and W.T. wrote the manuscript. All authors read and approved the final manuscript.

Notes

The views presented in this article do not necessarily reflect current or future opinion or policy of the U.S. Food and Drug Administration. Any mention of commercial products is for clarification and not intended as an endorsement.

The authors declare the following competing financial interest(s): R.R. is co-founder and co-director of ApconiX, an integrated toxicology and ion channel company that provides expert advice on nonclinical aspects of drug discovery and drug development to academia, industry, and not-for-profit organizations.

■ REFERENCES

(1) Justice, M. J., and Dhillon, P. (2016) Using the mouse to model human disease: increasing validity and reproducibility. *Dis. Models & Mech. 9*, 101−103.

(2) Macleod, M. R. (2014) Design animal studies better. *Nature 510*, 35.

(3) Annys, E., Billington, R., Clayton, R., Bremm, K.-D., Graziano, M., McKelvie, J., Ragan, I., Schwarz, M., van der Laan, J. W., Wood, C., Öberg, M., Wester, P., and Woodward, K. N. (2014) Advancing the 3Rs in regulatory toxicology − Carcinogenicity testing: Scope for harmonisation and advancing the 3Rs in regulated sectors of the European Union. *Regul. Toxicol. Pharmacol. 69*, 234−242.

(4) Hamburg, M. A. (2011) Advancing Regulatory Science. *Science 331*, 987−987.

(5) Dix, D. J., Houck, K. A., Martin, M. T., Richard, A. M., Setzer, R. W., and Kavlock, R. J. (2007) The ToxCast Program for Prioritizing Toxicity Testing of Environmental Chemicals. *Toxicol. Sci. 95*, 5−12.

DOI: 10.1021/acs.chemrestox.9b00288
Chem. Res. Toxicol. 2020, 33, 271−280

(6) Collins, F. S., Gray, G. M., and Bucher, J. R. (2008) Transforming Environmental Health Protection. *Science 319*, 906−907.
(7) Chen, M., Zhang, M., Borlak, J., and Tong, W. (2012) A Decade of Toxicogenomic Research and Its Contribution to Toxicological Science. *Toxicol. Sci. 130*, 217−228.
(8) Liu, Z., Huang, R., Roberts, R., and Tong, W. (2019) Toxicogenomics: A 2020 Vision. *Trends Pharmacol. Sci. 40*, 92−103.
(9) Li, A., Lu, X., Natoli, T., Bittker, J., Sipes, N., Subramanian, A., Auerbach, S., Sherr, D., and Monti, S. (2019) The Carcinogenome Project: In-vitro Gene Expression Profiling of Chemical Perturbations to Predict Long-Term Carcinogenicity. *Environ. Health Perspect. 127*, 047002.
(10) Ellinger-Ziegelbauer, H., Gmuender, H., Bandenburg, A., and Ahr, H. J. (2008) Prediction of a carcinogenic potential of rat hepatocarcinogens using toxicogenomics analysis of short-term in vivo studies. *Mutat. Res., Fundam. Mol. Mech. Mutagen. 637*, 23−39.
(11) Yu, D., Wu, L., Gill, P., Tolleson, W. H., Chen, S., Sun, J., Knox, B., Jin, Y., Xiao, W., Hong, H., Wang, Y., Ren, Z., Guo, L., Mei, N., Guo, Y., Yang, X., Shi, L., Chen, Y., Zeng, L., Dreval, K., Tryndyak, V., Pogribny, I., Fang, H., Shi, T., McCullough, S., Bhattacharyya, S., Schnackenberg, L., Mattes, W., Beger, R. D., James, L., Tong, W., and Ning, B. (2018) Multiple microRNAs function as self-protective modules in acetaminophen-induced hepatotoxicity in humans. *Arch. Toxicol. 92*, 845−858.
(12) Li, H.-H., Chen, R., Hyduke, D. R., Williams, A., Frötschl, R., Ellinger-Ziegelbauer, H., O'Lone, R., Yauk, C. L., Aubrecht, J., and Fornace, A. J. (2017) Development and validation of a high-throughput transcriptomic biomarker to address 21st century genetic toxicology needs. *Proc. Natl. Acad. Sci. U. S. A. 114*, E10881−E10889.
(13) Liu, Z., Delavan, B., Roberts, R., and Tong, W. (2018) Transcriptional Responses Reveal Similarities Between Preclinical Rat Liver Testing Systems. *Front. Genet. 9*, 74.
(14) Liu, Z. C., Fang, H., Borlak, J., Roberts, R., and Tong, W. D. (2017) In Vitro to In Vivo Extrapolation for Drug-Induced Liver Injury Using a Pair Ranking Method. *Altex-Alternatives to Animal Experimentation 34*, 399−408.
(15) Chen, B., and Butte, A. J. (2016) Leveraging big data to transform target selection and drug discovery. *Clin. Pharmacol. Ther. 99*, 285−297.
(16) Koudijs, K. K. M., Terwisscha van Scheltinga, A. G. T., Böhringer, S., Schimmel, K. J. M., and Guchelaar, H.-J. (2018) Personalised drug repositioning for Clear Cell Renal Cell Carcinoma using gene expression. *Sci. Rep. 8*, 5250.
(17) Kohonen, P., Parkkinen, J. A., Willighagen, E. L., Ceder, R., Wennerberg, K., Kaski, S., and Grafström, R. C. (2017) A transcriptomics data-driven gene space accurately predicts liver cytopathology and drug-induced liver injury. *Nat. Commun. 8*, 15932.
(18) Yeakley, J. M., Shepard, P. J., Goyena, D. E., VanSteenhouse, H. C., McComb, J. D., and Seligmann, B. E. (2017) A trichostatin A expression signature identified by TempO-Seq targeted whole transcriptome profiling. *PLoS One 12*, e0178302.
(19) Subramanian, A., Narayan, R., Corsello, S. M., Peck, D. D., Natoli, T. E., Lu, X., Gould, J., Davis, J. F., Tubelli, A. A., Asiedu, J. K., Lahr, D. L., Hirschman, J. E., Liu, Z., Donahue, M., Julian, B., Khan, M., Wadden, D., Smith, I. C., Lam, D., Liberzon, A., Toder, C., Bagul, M., Orzechowski, M., Enache, O. M., Piccioni, F., Johnson, S. A., Lyons, N. J., Berger, A. H., Shamji, A. F., Brooks, A. N., Vrcic, A., Flynn, C., Rosains, J., Takeda, D. Y., Hu, R., Davison, D., Lamb, J., Ardlie, K., Hogstrom, L., Greenside, P., Gray, N. S., Clemons, P. A., Silver, S., Wu, X., Zhao, W.-N., Read-Button, W., Wu, X., Haggarty, S. J., Ronco, L. V., Boehm, J. S., Schreiber, S. L., Doench, J. G., Bittker, J. A., Root, D. E., Wong, B., and Golub, T. R. (2017) A Next Generation Connectivity Map: L1000 Platform and the First 1,000,000 Profiles. *Cell 171*, 1437−1452.e17.
(20) Iskar, M., Zeller, G., Blattmann, P., Campillos, M., Kuhn, M., Kaminska, K. H., Runz, H., Gavin, A. C., Pepperkok, R., van Noort, V., and Bork, P. (2013) Characterization of drug-induced transcriptional modules: towards drug repositioning and functional understanding. *Mol. Syst. Biol. 9*, 662.
(21) Lamb, J., Crawford, E. D., Peck, D., Modell, J. W., Blat, I. C., Wrobel, M. J., Lerner, J., Brunet, J.-P., Subramanian, A., Ross, K. N., Reich, M., Hieronymus, H., Wei, G., Armstrong, S. A., Haggarty, S. J., Clemons, P. A., Wei, R., Carr, S. A., Lander, E. S., and Golub, T. R. (2006) The Connectivity Map: Using Gene-Expression Signatures to Connect Small Molecules, Genes, and Disease. *Science 313*, 1929−1935.
(22) Igarashi, Y., Nakatsu, N., Yamashita, T., Ono, A., Ohno, Y., Urushidani, T., and Yamada, H. (2015) Open TG-GATEs: a large-scale toxicogenomics database. *Nucleic Acids Res. 43*, D921−D927.
(23) Kuhn, M., Letunic, I., Jensen, L. J., and Bork, P. (2016) The SIDER database of drugs and side effects. *Nucleic Acids Res. 44*, D1075−D1079.
(24) Davis, A. P., Wiegers, T. C., Wiegers, J., Johnson, R. J., Sciaky, D., Grondin, C. J., and Mattingly, C. J. (2018) Chemical-Induced Phenotypes at CTD Help Inform the Predisease State and Construct Adverse Outcome Pathways. *Toxicol. Sci. 165*, 145.
(25) Heng, T. S. P., Painter, M. W., The Immunological Genome Project, C., Elpek, K., Lukacs-Kornek, V., Mauermann, N., Turley, S. J., Koller, D., Kim, F. S., Wagers, A. J., Asinovski, N., Davis, S., Fassett, M., Feuerer, M., Gray, D. H. D., Haxhinasto, S., Hill, J. A., Hyatt, G., Laplace, C., Leatherbee, K., Mathis, D., Benoist, C., Jianu, R., Laidlaw, D. H., Best, J. A., Knell, J., Goldrath, A. W., Jarjoura, J., Sun, J. C., Zhu, Y., Lanier, L. L., Ergun, A., Li, Z., Collins, J. J., Shinton, S. A., Hardy, R. R., Friedline, R., Sylvia, K., and Kang, J. (2008) The Immunological Genome Project: networks of gene expression in immune cells. *Nat. Immunol. 9*, 1091.
(26) Painter, M. W., Davis, S., Hardy, R. R., Mathis, D., and Benoist, C. (2011) Transcriptomes of the B and T Lineages Compared by Multiplatform Microarray Profiling. *J. Immunol. 186*, 3047−3057.
(27) Kidd, B. A., Wroblewska, A., Boland, M. R., Agudo, J., Merad, M., Tatonetti, N. P., Brown, B. D., and Dudley, J. T. (2016) Mapping the effects of drugs on the immune system. *Nat. Biotechnol. 34*, 47.
(28) Mav, D., Shah, R. R., Howard, B. E., Auerbach, S. S., Bushel, P. R., Collins, J. B., Gerhold, D. L., Judson, R. S., Karmaus, A. L., Maull, E. A., Mendrick, D. L., Merrick, B. A., Sipes, N. S., Svoboda, D., and Paules, R. S. (2018) A hybrid gene selection approach to create the S1500+ targeted gene sets for use in high-throughput transcriptomics. *PLoS One 13*, e0191105.
(29) Huang, D. W., Sherman, B. T., and Lempicki, R. A. (2009) Systematic and integrative analysis of large gene lists using DAVID bioinformatics resources. *Nat. Protoc. 4*, 44.
(30) Chen, M., Suzuki, A., Borlak, J., Andrade, R. J., and Lucena, M. I. (2015) Drug-induced liver injury: Interactions between drug properties and host factors. *J. Hepatol. 63*, 503−514.
(31) Varga, T., Czimmerer, Z., and Nagy, L. (2011) PPARs are a unique set of fatty acid regulated transcription factors controlling both lipid metabolism and inflammation(). *Biochim. Biophys. Acta, Mol. Basis Dis. 1812*, 1007−1022.
(32) Liu, Z., Delavan, B., Roberts, R., and Tong, W. (2017) Lessons Learned from Two Decades of Anticancer Drugs. *Trends Pharmacol. Sci. 38*, 852−872.
(33) Sirota, M., Dudley, J. T., Kim, J., Chiang, A. P., Morgan, A. A., Sweet-Cordero, A., Sage, J., and Butte, A. J. (2011) Discovery and Preclinical Validation of Drug Indications Using Compendia of Public Gene Expression Data. *Sci. Transl. Med. 3*, 96ra77−96ra77.
(34) Qu, X. A., and Rajpal, D. K. (2012) Applications of Connectivity Map in drug discovery and development. *Drug Discovery Today 17*, 1289−1298.
(35) Zeilinger, K., Freyer, N., Damm, G., Seehofer, D., and Knöspel, F. (2016) Cell sources for in vitro human liver cell culture models. *Exp. Biol. Med. (London, U. K.) 241*, 1684−1698.
(36) Zhang, J., Doshi, U., Suzuki, A., Chang, C.-W., Borlak, J., Li, A. P., and Tong, W. (2016) Evaluation of multiple mechanism-based toxicity endpoints in primary cultured human hepatocytes for the identification of drugs with clinical hepatotoxicity: Results from 152

DOI: 10.1021/acs.chemrestox.9b00288
Chem. Res. Toxicol. 2020, 33, 271−280

marketed drugs with known liver injury profiles. *Chem.-Biol. Interact. 255*, 3−11.
(37) Kotsampasakou, E., Montanari, F., and Ecker, G. F. (2017) Predicting drug-induced liver injury: The importance of data curation. *Toxicology 389*, 139−145.
(38) Lee, W. M. (2003) Drug-Induced Hepatotoxicity. *N. Engl. J. Med. 349*, 474−485.
(39) Chen, M., Bisgin, H., Tong, L., Hong, H., Fang, H., Borlak, J., and Tong, W. (2014) Toward predictive models for drug-induced liver injury in humans: are we there yet? *Biomarkers Med. 8*, 201−213.
(40) Chen, M., Hong, H., Fang, H., Kelly, R., Zhou, G., Borlak, J., and Tong, W. (2013) Quantitative Structure-Activity Relationship Models for Predicting Drug-Induced Liver Injury Based on FDA-Approved Drug Labeling Annotation and Using a Large Collection of Drugs. *Toxicol. Sci. 136*, 242−249.
(41) Hong, H., Thakkar, S., Chen, M., and Tong, W. (2017) Development of Decision Forest Models for Prediction of Drug-Induced Liver Injury in Humans Using A Large Set of FDA-approved Drugs. *Sci. Rep. 7*, 17311.
(42) Liu, Z., Shi, Q., Ding, D., Kelly, R., Fang, H., and Tong, W. (2011) Translating Clinical Findings into Knowledge in Drug Safety Evaluation - Drug Induced Liver Injury Prediction System (DILIps). *PLoS Comput. Biol. 7*, e1002310.
(43) Zhang, M., Chen, M., and Tong, W. (2012) Is Toxicogenomics a More Reliable and Sensitive Biomarker than Conventional Indicators from Rats To Predict Drug-Induced Liver Injury in Humans? *Chem. Res. Toxicol. 25*, 122−129.
(44) Wu, L., Liu, Z., Auerbach, S., Huang, R., Chen, M., McEuen, K., Xu, J., Fang, H., and Tong, W. (2017) Integrating Drug's Mode of Action into Quantitative Structure−Activity Relationships for Improved Prediction of Drug-Induced Liver Injury. *J. Chem. Inf. Model. 57*, 1000−1006.
(45) Tao, L., and Reese, T. A. (2017) Making Mouse Models That Reflect Human Immune Responses. *Trends Immunol. 38*, 181−193.

DOI: 10.1021/acs.chemrestox.9b00288
Chem. Res. Toxicol. 2020, 33, 271−280